

# The Relative Impact of Stratospheric Photochemical Production on Tropospheric NO<sub>y</sub> Levels: A Model Study

P. S. KASIBHATLA,<sup>1,2</sup> H. LEVY II,<sup>3</sup> W. J. MOXIM,<sup>3</sup> AND W. L. CHAMEIDES<sup>1</sup>

The 11-level Geophysical Fluid Dynamics Laboratory (GFDL) global chemical transport model has been used to assess the impact of stratospheric NO<sub>x</sub> production on tropospheric reactive nitrogen (NO<sub>y</sub>) concentrations. A temporally varying source function was constructed using specified two-dimensional, monthly average O<sub>3</sub>, N<sub>2</sub>O, temperature, and surface pressure data generated by the GFDL "SKYHI" model. The calculated yearly NO<sub>y</sub> production rate is 0.64 Tg N (0.64 × 10<sup>12</sup> g N). A wet removal scheme, which distinguishes between stable and convective rain based on the bulk Richardson number, is introduced. Simulations have been performed with a simplified chemical mechanism which fractionates NO<sub>y</sub> into soluble and insoluble species. The role of peroxyacetyl nitrate (PAN) in determining the impact of stratospheric injection on the tropospheric NO<sub>y</sub> budget is studied by comparing results of simulations with and without PAN chemistry. We conclude that (1) the stratospheric source is too small to account for background surface NO<sub>y</sub> concentrations observed in the remote (i.e., regions a few thousand kilometers from continental source regions) troposphere. Surface NO<sub>y</sub> mixing ratios seldom exceed 10 parts per trillion by volume (pptv) in the model northern hemisphere and are always below 20 pptv. Together, fossil fuel combustion emissions and stratospheric injection account for less than 10% of observed surface nitrate concentrations in the remote tropical Pacific. (2) The impact of the stratospheric source is comparable to that of the fossil fuel combustion source in terms of NO<sub>y</sub> mixing ratios in the northern hemisphere at the 500 mbar model level and is more important in the middle and high latitudes of the southern hemisphere. At the 315 mbar model level the stratospheric source contribution to NO<sub>y</sub> levels is more important than that of the fossil fuel source at all latitudes, except in the tropics. However, substantial contributions from other NO<sub>y</sub> sources are needed to explain observations in the remote middle and upper troposphere. (3) Inclusion of PAN chemistry has the effect of increasing model-calculated surface NO<sub>y</sub> mixing ratios in the northern hemisphere middle and high latitudes by factors of 1.5-3 during winter/spring and by factors of 2-4 during summer/fall. Surface NO<sub>y</sub> mixing ratios in the southern hemisphere show a smaller increase due to slower rates of PAN formation. This is a direct result of lower hydrocarbon concentrations in the southern hemisphere.

## INTRODUCTION

The importance of reactive nitrogen compounds (NO<sub>y</sub>) in atmospheric chemistry over a variety of spatial and temporal scales has long been recognized. Nitrogen oxides (NO<sub>x</sub> = NO + NO<sub>2</sub>) play a major role in determining the global oxidizing power of the troposphere by controlling tropospheric O<sub>3</sub> [Crutzen, 1974] and OH levels [Levy, 1971]. Thus they may have a significant influence on global climate through their indirect impact on the rate of removal of greenhouse gases from the atmosphere. NO<sub>x</sub> has also been shown to be an important precursor to urban photochemical smog formation [Leighton, 1961], and HNO<sub>3</sub> is one of the two important acidic components of acid rain [National Research Council (NRC) 1983]. In addition, nitrate is an important nutrient to oceanic ecosystems [Ryther and Dunstan, 1971].

A comprehensive knowledge of the key factors affecting NO<sub>y</sub> distributions is essential if one attempts to isolate the influence of humans on atmospheric chemistry in particular and on global climate in general. Our present understanding of the factors controlling the distribution of NO<sub>y</sub> is ex-

remely limited due to the sparsity of available observational data, especially in remote regions of the world. In this context, models provide us with a valuable tool to synthesize the knowledge gained from limited field studies and to extrapolate the data to more representative global scenarios.

A fundamental question, which remains largely unanswered, relates to the nature, magnitude, and spatial and temporal variation of the various sources of NO<sub>y</sub>. Levy and Moxim [1989] simulated the global distribution and deposition of NO<sub>y</sub> emitted by fossil fuel combustion. These emissions are mainly concentrated in the northern mid-latitudes, with a global annual source strength of approximately 21 Tg N (21 × 10<sup>12</sup> g N). Their analysis showed that while these emissions were sufficient to account for a large fraction of observed surface NO<sub>y</sub> levels near source regions in the northern hemisphere, they were insufficient to account for more than ~10% of observed background levels in the remote tropics and in the southern hemisphere. They speculated that other possible sources of NO<sub>x</sub> such as biomass burning, production by lightning, biogenic emissions, and stratospheric injection may make important contributions to the tropospheric NO<sub>y</sub> budget. With the exception of the stratospheric source these sources are inherently difficult to quantify owing to their nature and due to their geographical distribution.

On the basis of a simulation with an idealized source, Levy *et al.* [1980] hypothesized that the stratospheric source could account for at least half the NO<sub>y</sub> present in the remote tropics and in the southern hemisphere. Liu *et al.* [1980] carried this one step further, arguing that downward transport of NO<sub>x</sub> produced in the stratosphere and subsequent

<sup>1</sup>School of Earth and Atmospheric Sciences, Georgia Institute of Technology, Atlanta.

<sup>2</sup>Currently visiting scientist at Geophysical Fluid Dynamics Laboratory, Princeton University, Princeton, New Jersey.

<sup>3</sup>Geophysical Fluid Dynamics Laboratory, Princeton University, Princeton, New Jersey.

Copyright 1991 by the American Geophysical Union.

Paper number 91JD01665.  
0148-0227/91/91JD-01665\$05.00

photochemical production of O<sub>3</sub> in the upper troposphere could be a significant source of tropospheric O<sub>3</sub>. Their calculations used the NO<sub>y</sub> fields predicted by *Levy et al.* [1980], along with semiempirically derived NO<sub>x</sub>/NO<sub>y</sub> ratios from *Kley et al.* [1981]. On the other hand, *Logan* [1983] argued that the stratospheric flux was too small to have a significant impact on tropospheric NO<sub>y</sub> levels and suggested that *Levy et al.* [1980] had used unrealistically long rainout lifetimes in their model calculations. Recent analysis of surface observations in the tropical Pacific also suggests that the stratospheric source may have a minimal impact on surface NO<sub>y</sub> concentrations [*Savoie et al.*, 1989].

In the above mentioned model studies, *Levy et al.* [1980] and *Levy and Moxim* [1989] treated the collection of reactive nitrogen compounds as a single species, namely, NO<sub>y</sub>. By using effective dry and wet removal coefficients for NO<sub>y</sub>, an attempt was made to implicitly capture the effect of chemical transformations and removal of individual species on the distribution and deposition of total reactive nitrogen. A problem arises, however, in arriving at a priori estimates of wet and dry removal coefficients for an arbitrary source distribution. Even for a particular source function, such as the fossil fuel combustion source, where observed deposition fluxes provide a constraint against which model parameters may be adjusted over source regions, it is by no means certain that removal rates will be calculated "correctly" in regions remote from the source region. The approach taken in this paper is therefore a more fundamental one. We explicitly treat NO<sub>x</sub>, HNO<sub>3</sub>, and PAN as transported species, using a simplified chemical scheme to calculate chemical production and destruction rates for each of these species.

This study focuses on a reexamination of the potential impact of stratospheric photochemical NO<sub>x</sub> production on tropospheric NO<sub>y</sub> levels. We therefore present an analysis of the results of a set of model simulations with this stratospheric source alone. An assessment of the relative impact of this small source (0.64 Tg N yr<sup>-1</sup>) is provided by comparing model results with available observations of tropospheric NO<sub>y</sub> mixing ratios and deposition fluxes. Similar studies with other individual sources are presently under way and will be discussed in future papers.

## 2. BRIEF DESCRIPTION OF THE MODEL

The global chemical transport model (GCTM) has a horizontal resolution of ~265 km and 11 vertical levels at standard pressures of 990, 940, 835, 685, 500, 315, 190, 110, 65, 38, and 10 mbar. The model is driven by 6-hour time-averaged wind and total precipitation fields derived from a 1-year integration of a parent general circulation model (GCM) [*Manabe et al.*, 1974; *Manabe and Holloway*, 1975]. The meteorological features of the GCM have been the subject of many previous studies, and the interested reader may wish to refer to the paper by *Mahlman and Moxim* [1978] for a comprehensive list of references pertaining to the GCM and an encapsulated review of the GCM climatology pertinent to this study. However, a few remarks on the dynamics of stratosphere-troposphere exchange processes in the model are appropriate here. The meridional circulation in the GCM consists of a 3-cell troposphere, a 2-cell northern hemisphere stratosphere, and a 3-cell southern hemisphere stratosphere, with midstratospheric flow from the summer to

the winter hemisphere. A detailed description of the simulated dynamics in the stratosphere is given by *Manabe and Mahlman* [1976]. The tropopause appears at the proper altitudes, and its poleward downward slope agrees well with observations. *Mahlman and Moxim* [1978] found in their mid-latitude instantaneous source experiment that the global mean vertical transport across the tropopause is dominated by eddy transport. At particular latitudes, however, the eddy transport is of the same order of magnitude as the mean transport, reflecting the fact that eddy transport is predominantly downward, while the mean transport may be upward or downward. In their study, strongest downward eddy cross-tropopause fluxes occur near 50°–60°N during March–May, associated with upper tropospheric cyclogenesis, while strongest downward zonal mean fluxes occur near 35°–45°N during December–February. An analysis of the transport of an ozonelike tracer by *Mahlman et al.* [1980] found that the annually averaged northern hemisphere cross-tropopause flux was approximately 1.8 times larger than the corresponding flux in the model southern hemisphere. Their study also suggests that the model may considerably underestimate cross-tropopause tracer fluxes in the southern hemisphere.

The GCTM incorporates parameterizations for approximating horizontal sub-grid-scale transport, vertical mixing by dry and moist convection, and vertical mixing in the boundary layer under conditions of large-scale stability. Dry deposition is calculated based on the assumption of a balance between surface deposition and the turbulent flux in the bottom half of the lowest level in the model. The deposition velocities used in the model (indicated in section 3) reflect measured deposition velocities of individual reactive nitrogen species. A more detailed description of these and other features of the GCTM can be found in studies by *Mahlman and Moxim* [1978], *Levy et al.* [1982, 1985], and *Levy and Moxim* [1989]. A significant change in the present application of the model is the manner in which wet removal rates are calculated. Our current scheme, the main ideas of which are borrowed from *Giorgi and Chameides* [1986], is outlined in more detail below.

Consider a column of grid boxes in which precipitation occurs. Let  $A_B$  and  $H$  represent the cross-sectional area and height of the column, respectively, and  $F$  represent the fraction of the cross-sectional area over which precipitation occurs. We now assume that for a highly soluble tracer (such as HNO<sub>3</sub>),  $F$  is also the fraction of the tracer originally present in a box that is removed during a precipitation event. Wet deposition rates for a highly soluble tracer, at each time step and each grid box, can then be calculated as

$$\left. \frac{\partial R}{\partial t} \right|_{(\text{wet})} = \frac{-FR}{\Delta t}, \quad (1)$$

where  $R$  is the tracer mixing ratio. We now have to determine  $F$ . If  $L$  is the liquid water content of the "cloud" and  $Q$  is the precipitation rate averaged over the column cross-sectional area, the volume of cloud,  $V_c$ , is

$$V_c = \frac{A_B Q \Delta t \rho}{L}, \quad (2)$$

where  $\rho$  is the density of liquid water. We use the term cloud in the same sense as *Giorgi and Chameides* [1986], i.e., to

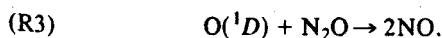
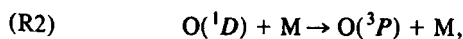
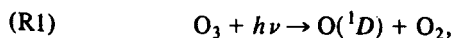
refer to that fraction of the grid where precipitation is occurring. The fraction of the column cross-sectional area over which precipitation and therefore wet removal occurs is then

$$F = \frac{V_c}{HA_B} = \frac{Q\Delta t\rho}{LH} \quad (3)$$

Equations (1) and (3) together represent the parameterization for wet removal, based on GCM-derived precipitation intensity fields, that is used in the GCTM for a highly soluble species. In the actual application of the scheme the height  $H$  is specified to be the height of the top of the 685 mbar layer in the model except when there is convective instability as determined by the moist Richardson number ( $Ri_m$ ) calculated at the 500 and 315 mbar levels. The mathematical expression used to calculate  $Ri_m$  is given by *Levy et al.* [1982]. If  $Ri_m$  is less than 0.25 for the 315 mbar level, wet removal is assumed to occur from the ground to the top of the 315 mbar layer. Similarly, if  $Ri_m$  is greater than 0.25 for the 315 mbar level but less than 0.25 for the 500 mbar level, wet removal is assumed to occur from the ground to the top of the 500 mbar layer. We use the term "convective rain" to characterize precipitation events for which  $Ri_m$  is less than 0.25 at the 315 or 500 mbar model levels. All other precipitation events are termed "nonconvective." Values for  $L$  are the same as those used by *Giorgi and Chameides* [1986], with  $L = 2 \times 10^{-6} \text{ g cm}^{-3}$  for convective rain and  $L = 0.5 \times 10^{-6} \text{ g cm}^{-3}$  for nonconvective rain. We have performed some preliminary tests with this scheme by simulating the global distribution of NO<sub>y</sub> resulting from fossil fuel combustion emissions only. These simulations indicate that model-calculated wet deposition fluxes agree with observed wet deposition fluxes in North America and Europe (where fossil fuel combustion emissions dominate the NO<sub>y</sub> budget) at least as well as previous calculations by *Levy and Moxim* [1989] in which a different wet removal scheme was used. In addition, nitrate wet deposition fluxes at sites in the North Atlantic which are mainly impacted by fossil fuel combustion are well simulated.

### 3. DESIGN OF THE EXPERIMENTS

NO is produced in the stratosphere by the following reaction sequence:



Reaction (R1) generates highly reactive atomic oxygen, which is either quenched by collision with molecular oxygen and nitrogen (reaction (R2)) or reacts with nitrous oxide (transported to the stratosphere from the troposphere) to yield two molecules of NO per atom of oxygen reacting with N<sub>2</sub>O (reaction (R3)). Using monthly and zonally averaged O<sub>3</sub> and N<sub>2</sub>O fields (shown in Figure 1 for the months of January and July), along with corresponding temperature and surface pressure data from the GFDL "SKYHI" GCM which has a higher vertical resolution [*Hamilton and Mahlman*, 1988], we have calculated diurnally averaged NO production rates for the middle of each month based on (R1)–(R3). Kinetic data used in the calculations were ob-

tained from *DeMore et al.* [1990]. The calculated NO production rates for 4 months representing winter, spring, fall, and summer are shown in Figure 2. The seasonal variation of the NO production rate is clearly seen, with maximum production occurring in the summer hemisphere. Maximum production rates ( $\sim 200\text{--}240 \text{ molecules cm}^{-3} \text{ s}^{-1}$ ) occur near the equator at approximately 10 mbar. The calculated annual NO production rate is 0.64 Tg N. This estimate is consistent with recent estimates of 0.4–0.7 Tg N/yr [*Crutzen and Schmailzl*, 1983] and 0.7 Tg N/yr [*Legrand et al.*, 1989]. *Jackman et al.* [1980] have argued that the production of NO by galactic cosmic rays in the lower stratosphere and upper troposphere is comparable to the production of NO by N<sub>2</sub>O oxidation at latitudes poleward of  $\sim 50^\circ$ . On a global scale, however, N<sub>2</sub>O oxidation is the dominant stratospheric NO<sub>x</sub> source. As we shall see later, our conclusions regarding the tropospheric impact of the stratospheric source are mainly drawn by comparing model results with measurements in the remote tropics and subtropics. Our conclusions therefore are not significantly affected by the fact that we have considered only the photochemical NO<sub>x</sub> source in the present study. In addition, NO<sub>x</sub> emitted in the exhaust fumes of jet aircraft may contribute locally to NO<sub>y</sub> levels in mid-latitudes, but we have made no attempt to quantify the effect of this source. Calculated source strengths were gridded to the GCTM grid and specified in the form of a "lookup" table in the model. We should point out that although the top model full-level is at 10 mbar, the top model layer extends from  $\sim 27$  mbar to the top of the atmosphere. Daily NO production rates were calculated in the GCTM by time-interpolating between appropriate table values.

The chemical partitioning of NO<sub>y</sub> into soluble and insoluble fractions was calculated using a simple chemical scheme and using NO<sub>x</sub> and HNO<sub>3</sub> as surrogates for insoluble and soluble reactive nitrogen species, respectively. Details of the chemical scheme are given in the appendix. Deposition velocities for HNO<sub>3</sub> ( $1.0 \text{ cm s}^{-1}$  over land,  $0.5 \text{ cm s}^{-1}$  over ocean) and for NO<sub>x</sub> ( $0.2 \text{ cm s}^{-1}$  over land,  $0.0 \text{ cm s}^{-1}$  over ocean) were selected based on the annual average of available measurements over land [*Cadle et al.*, 1985; *Huebert and Robert*, 1985; *Wesely et al.*, 1982; *Walcek et al.*, 1986; *Voldner et al.*, 1986]. Calculation of wet deposition involves treating NO<sub>x</sub> as an insoluble species and using (1) and (3) to determine HNO<sub>3</sub> removal rates. We treat this simulation as our base case simulation and will hereinafter refer to it as the case 1 experiment.

We next focus on the role of long-lived, reservoir organic species formation in determining tropospheric NO<sub>y</sub> concentrations. The chemistry involved in the formation and destruction of these organic constituents is extremely complex [*Madronich and Calvert*, 1990]. In addition, many of the reaction rates and products are not well characterized. In this study we therefore attempt to provide only a zeroth-order analysis of the impact of such a sequestration on the tropospheric NO<sub>y</sub> burden. We use PAN as a surrogate for the organic NO<sub>y</sub> species and calculate PAN production and destruction rates using a specified hydrocarbon distribution. PAN production is assumed to occur only at or below the 190 mbar model level equatorward of  $45^\circ$  latitude and at or below the 315 mbar model level poleward of  $45^\circ$  latitude. Our scheme considers six reactions:



RECEIVED FEBRUARY 1995

5107

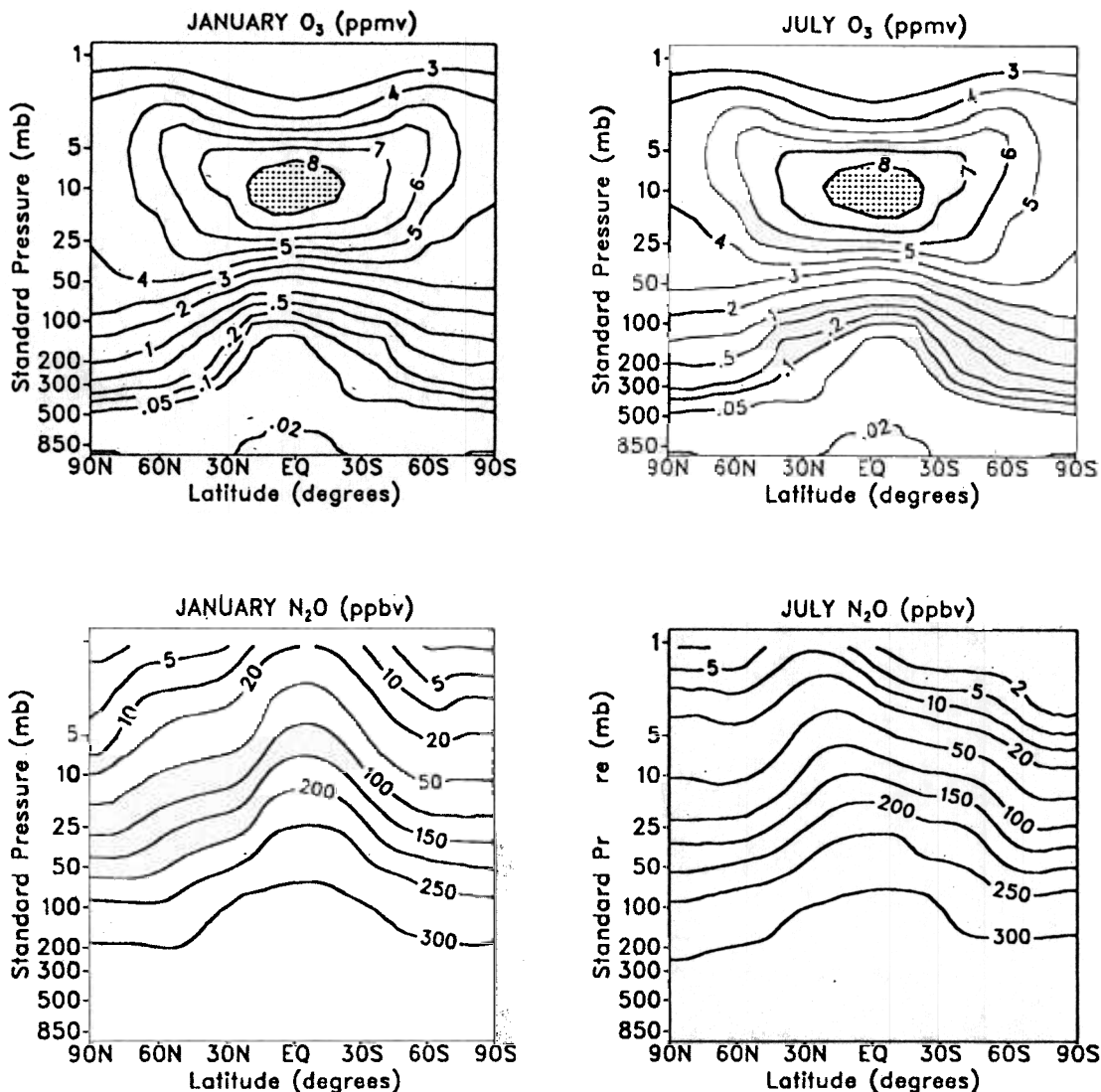
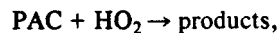
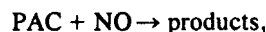


Fig. 1. Monthly average O<sub>3</sub> (ppmv) and N<sub>2</sub>O (ppbv) fields used in the calculation of the stratospheric NO<sub>x</sub> source. Contour levels for O<sub>3</sub> are 0.02, 0.05, 0.1, 0.2, 0.5, 1, 2, 3, 4, 5, 6, 7, and 8 ppmv. Contour levels for N<sub>2</sub>O are 2, 5, 10, 20, 50, 100, 150, 200, 250, and 300 ppbv.



where HC and PAC refer to hydrocarbons and peroxyacetyl radical, respectively. By assuming that PAC is in photochemical equilibrium, the production rate of PAN is given by

$$P_{\text{PAN}}^s = k_{P2} \left[ \frac{k_{P1}n(\text{HC})n(\text{OH})}{k_{P2}n(\text{NO}_2) + k_{P3}n(\text{NO}) + k_{P4}n(\text{HO}_2)} \right] \frac{n(\text{NO}_2)}{n(\text{NO}_x)} n(\text{NO}_x^s), \quad (4)$$

where the  $n$  coefficient represents number density and  $k_j$  is the specific reaction rate for reaction  $j$ . Number densities of OH, HO<sub>2</sub>, NO, NO<sub>2</sub>, and NO<sub>x</sub> are calculated using the scheme described in the appendix, and the superscript "s" refers to quantities derived in the transport model from the stratospheric source alone. Similarly, the PAN destruction rate is

$$L_{\text{PAN}}^s = \left[ k_{P6}n(\text{OH}) + \frac{k_{P5}\{k_{P3}n(\text{NO}) + k_{P4}n(\text{HO}_2)\}}{k_{P2}n(\text{NO}_2) + k_{P3}n(\text{NO}) + k_{P4}n(\text{HO}_2)} \right] n(\text{PAN}^s). \quad (5)$$

In this study we use ethane as a surrogate for all hydrocarbons which produce PAC and specify uniform ethane mixing ratios of 2 and 0.4 (parts per billion by volume) ppbv in the northern and southern hemispheres, respectively,

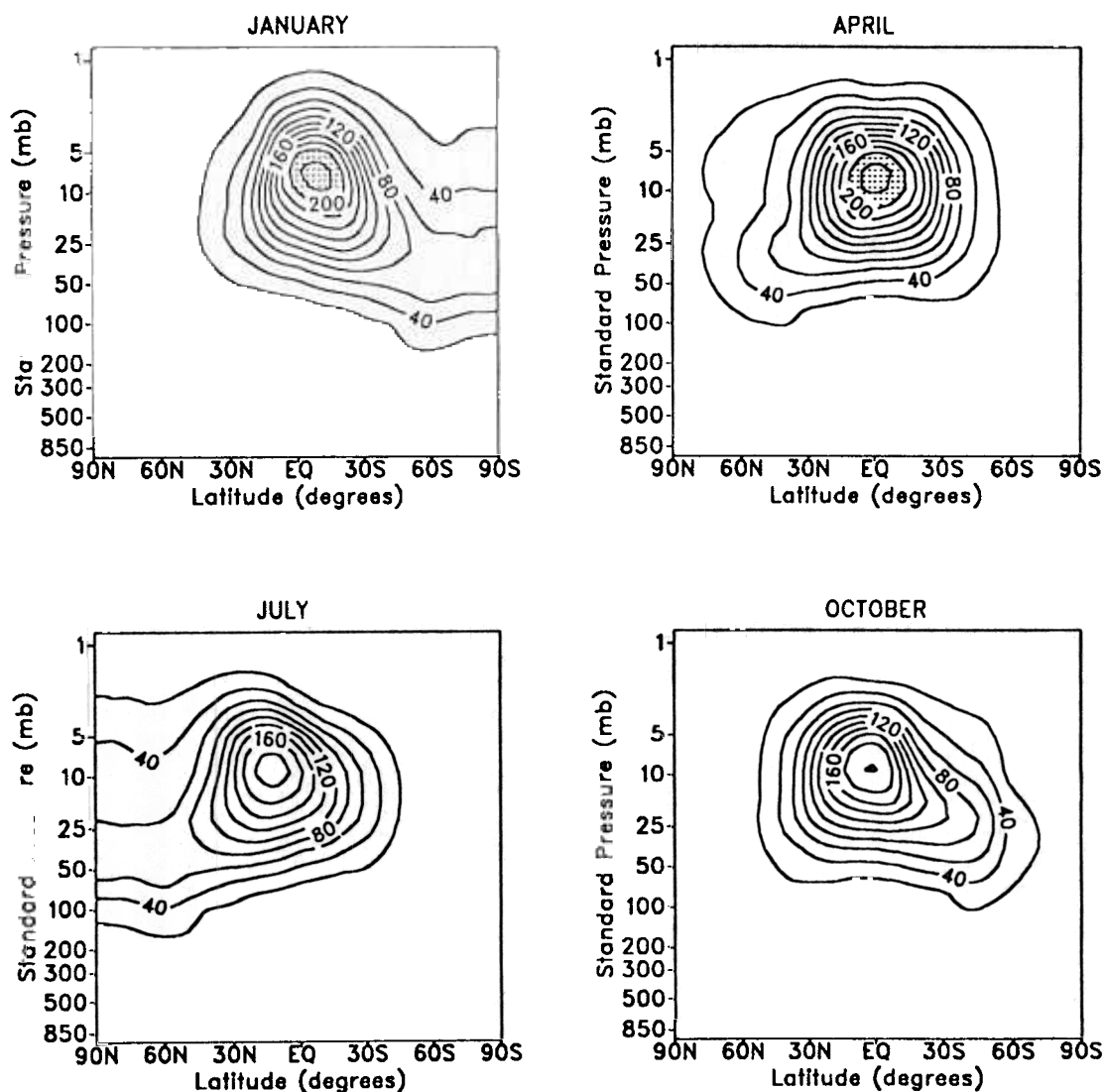


Fig. 2. Calculated NO production rates ( $\text{molecules cm}^{-3} \text{s}^{-1}$ ) for indicated months. Contour levels range from 20 to 220, in increments of 20.

based on measured hydrocarbon concentrations in the background atmosphere [Singh and Zimmerman, 1991; Rudolph, 1988]. Kinetic data for (P1) is obtained from DeMore *et al.* [1990], while rate constants recommended by Atkinson and Lloyd [1984] are used for (P2), (P3), and (P5). It should be noted that the rate of thermal decomposition of PAN (reaction (P5)) is highly temperature sensitive ( $k_{p5} = 1.95 \times 10^{16} e^{-13543/T} \text{ s}^{-1}$ ). PAN formation at low temperatures therefore provides a pathway by which some of the NO<sub>y</sub> can be sequestered in a stable form. Subsequent long-range transport of PAN can then serve as a potentially important source of NO<sub>y</sub> in the remote troposphere. There is some uncertainty regarding the products of (P6). In this study we assume (P6) to be a chemical source of NO<sub>x</sub>, with  $k_{p6} = 1.23 \times 10^{-12} e^{-651/T} \text{ cm}^3 \text{ molecules}^{-1} \text{ s}^{-1}$  [Singh *et al.*, 1991a]. We further assume that PAN has neither dry nor wet sinks, thus providing an upper limit of the impact of tropospheric PAN production on the global NO<sub>y</sub> burden resulting from stratospheric injection. This model experiment will be referred to as case 2.

The results of our model calculations are presented in section 4. Section 4.1 focuses on the zonal mean mixing ratio

fields from the case 1 experiment, while the case 2 simulation is compared with the case 1 experiment in section 4.2. A more detailed analysis of surface and middle and upper tropospheric NO<sub>y</sub> mixing ratios is presented in sections 4.3 and 4.4.

#### 4. RESULTS OF THE EXPERIMENTS

The GCTM case 1 simulation was initialized with a one-dimensional NO<sub>y</sub> profile, varying from  $\sim 50$  pptv at the surface to  $\sim 17.5$  ppbv at 10 mbar. On the model start-up date of October 1 this initial NO<sub>y</sub> field was partitioned into NO<sub>x</sub> and HNO<sub>3</sub> on the basis of chemical production and destruction rates calculated using the simple chemical scheme described in the appendix. The model was integrated for a period of 64 months, at which time globally and annually averaged sources and sinks were essentially in balance for both NO<sub>x</sub> and HNO<sub>3</sub>. The case 2 simulation was initialized with NO<sub>x</sub> and HNO<sub>3</sub> distributions obtained after integrating the case 1 simulation for 28 months. In addition, a uniform background mixing ratio of 1 pptv was used to initialize

ACCEPTED MANUSCRIPT

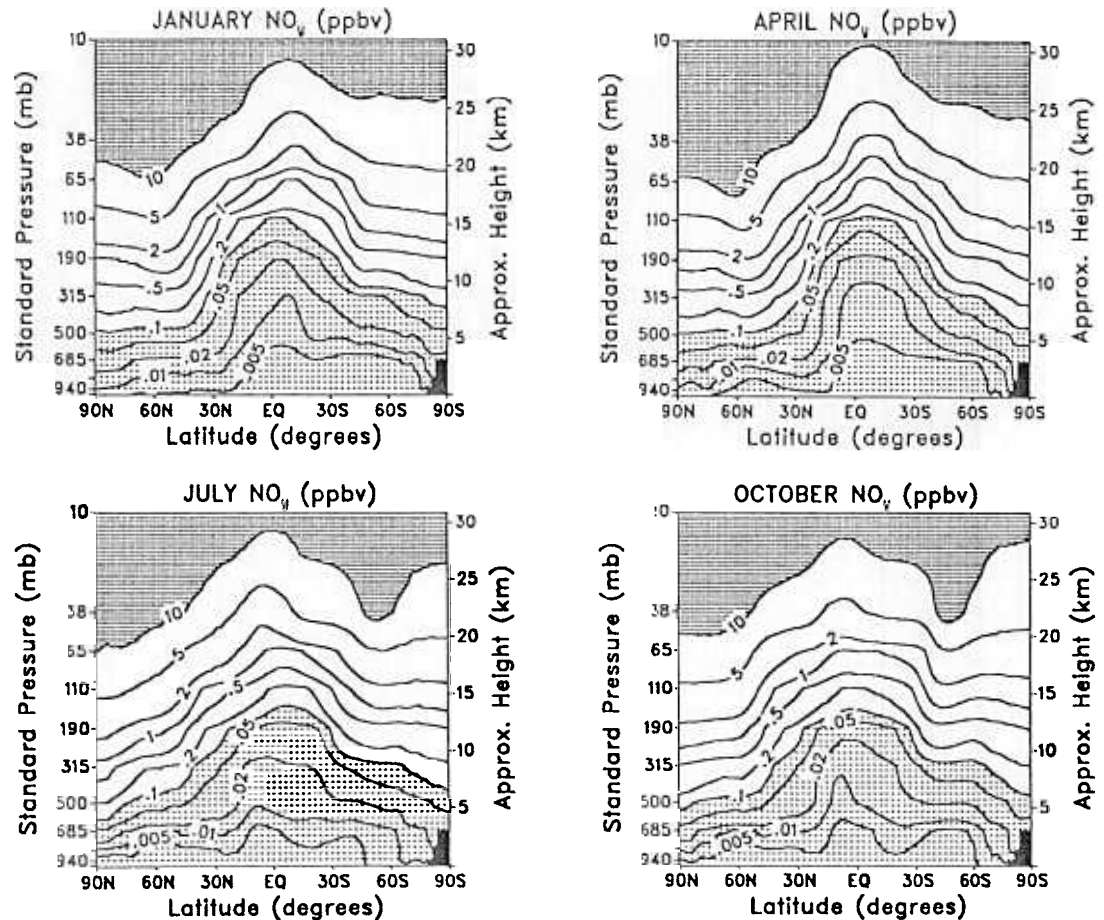


Fig. 3. Monthly average, zonal mean NO<sub>y</sub> mixing ratios (ppbv) for indicated months from the case 1 experiment. Contour levels are logarithmic.

PAN, and the model was integrated for a period of 36 months. In the rest of this paper we will focus on the resulting steady state distributions, and hence all subsequent discussions will refer to model fields from the last 12 months of each experiment. While this study will be mainly confined to an analysis of the resulting tropospheric mixing ratio fields and comparisons of these model fields with available observations, we will also examine the zonal mean distribution of NO<sub>y</sub> and its constituents from the midstratosphere to the surface.

#### 4.1. Zonal Mean Mixing Ratio Fields From the Case 1 Experiment

Monthly average, zonal mean NO<sub>y</sub> fields from the case 1 experiment are shown in Figure 3 for the months of January, April, July, and October. The familiar feature of poleward-downward sloping isopleths is seen, with higher mixing ratios occurring poleward and lowest values at or near the equator. Seasonal variations in mid-latitude tropospheric mixing ratios are evident, with maximum values occurring during winter and spring in each hemisphere. Another interesting feature is the steepening of tracer mixing ratio isolines at high northern latitudes during the transition from spring to summer. *Mahlman and Moxim* [1978] put forward the diagnostic interpretation that this was due to a diminished degree of self-cancellation between mean and eddy effects during the seasonal transition. A similar feature is not evident in the

model southern hemisphere and appears to be a model defect.

The stratospheric source appears to be significant relative to the fossil fuel combustion source in terms of middle-upper tropospheric NO<sub>y</sub> mixing ratios in mid-latitudes, especially during winter and spring. At the 500 mbar model level the stratospheric source yields zonal mean NO<sub>y</sub> mixing ratios of approximately 100 pptv in the northern hemisphere mid-latitudes. This is comparable to estimates of zonal mean NO<sub>y</sub> resulting from the combustion source alone [*Levy and Moxim*, 1989]. In addition, model NO<sub>y</sub> mixing ratios from the stratospheric source (200–500 pptv) are a factor of 2–10 higher than those produced by the combustion source in the northern mid-latitudes at 315 mbar. The stratospheric source is also clearly more important than the fossil fuel combustion emission source in the southern hemisphere midtroposphere as evidenced by the very low NO<sub>y</sub> levels (2–10 pptv) calculated by *Levy and Moxim* [1989] in their fossil fuel combustion experiment. The results from the case 1 simulation also seem to indicate that the stratospheric source has only a small impact on surface NO<sub>y</sub> where model mixing ratios are generally below 5 pptv, with slightly higher values at high latitudes.

A closer examination of Figure 3 also reveals a significant interhemispheric asymmetry in midtropospheric mixing ratios, with higher mixing ratios in the northern hemisphere. While the annually averaged NO<sub>y</sub> source has no interhemi-

spheric asymmetry, some asymmetries arise due to differences in wet and dry removal rates in the two hemispheres. However, the major difference between the two hemispheres is the considerably weaker poleward-downward transport from the production region in the middle stratosphere to the lower stratosphere in the model southern hemisphere [Mahlman *et al.*, 1980]. While this asymmetry is to be expected on the basis of stratospheric dynamics, it may be exaggerated in this model.

Table 1 shows a comparison between LIMS-derived (limb infrared monitor of the stratosphere) NO<sub>y</sub> for January 1979 [World Meteorological Organization (WMO) 1985] and model-simulated NO<sub>y</sub> at 50 mbar. NO<sub>y</sub> mixing ratios in the northern hemisphere extratropical stratosphere are reasonably well simulated, though the slight overestimate in the tropics and underestimate in the mid-latitudes indicate that the slopes of the mixing ratio isopleths are too flat. Mahlman *et al.* [1986] obtained a similar result in their simulation of stratospheric N<sub>2</sub>O. They found that observed meridional slopes of mixing ratio isolines were steeper than those simulated by the model by about 30%. Their analysis showed that this discrepancy was caused by the fact that the magnitude of meridional gradient of net diabatic heating was underestimated in the model, leading them to conclude that the magnitude of the dynamical drive in the model stratosphere was too weak. The model underestimates NO<sub>y</sub> in the high latitude lower stratosphere of the southern hemisphere, again suggesting that poleward-downward transport from the middle stratosphere is too weak in the model southern hemisphere.

It is also interesting to compare model results from this experiment with those from Mahlman *et al.* [1980] involving an ozonelike tracer. In that study the latitudinal tracer gradient at the 10 mbar model level is maintained by relatively fast photochemistry, with the result that maximum mixing ratios at the top model level occur in the tropics (see Figure 3.3, Mahlman *et al.* [1980]). In sharp contrast in the present study, highest NO<sub>y</sub> mixing ratios at 10 mbar occur at high latitudes, reflecting the dominant role of transport processes in establishing the latitudinal NO<sub>y</sub> gradient at that level. In spite of this striking dissimilarity in tracer distributions at the top model level, slopes of the mixing ratio isopleths in the lower stratosphere are remarkably similar in the two studies. This is due to the fact that in both studies it is the average stratification of tracer between the middle and lower stratosphere that determines the tracer structure in this region [Mahlman *et al.*, 1980].

Zonally averaged NO<sub>x</sub> and HNO<sub>3</sub> distributions for January and July are shown in Figure 4. While HNO<sub>3</sub> mixing ratios are 2–3 times higher than those of NO<sub>x</sub> in the extratropical lower stratosphere, NO<sub>x</sub> is more abundant above the 38 mbar model level in the equatorial stratosphere due to the fact that the local NO<sub>x</sub> photochemical source is largest in this region and also due to the relatively rapid rate of HNO<sub>3</sub> photolysis in this region. In the middle and upper extratropical troposphere, however, HNO<sub>3</sub> mixing ratios are significantly higher than NO<sub>x</sub> levels. For example, HNO<sub>3</sub> mixing ratios range from 50 pptv to greater than 200 pptv, while the corresponding NO<sub>x</sub> mixing ratios are 20–100 pptv poleward of 30°N in January at the 315 mbar model level. This can be explained on the basis of the fact that the rate of conversion of HNO<sub>3</sub> to NO<sub>x</sub> decreases rapidly in going from the stratosphere to the middle troposphere. Scavenging of

TABLE 1. Comparison of Model Results With LIMS-Derived Lower Stratospheric NO<sub>y</sub> for January

Location	Observation*	Model†
64°S	9–10	5–6
48°S	~8	~5
32°S	~6	3–4
16°S	~2	1–2
Equator	<2	~2
16°N	~3	4–5
32°N	~9	6–7
48°N	~13	10–11

Observations are for January 1979, at approximately 50 mbar (see Figures 10–68, WMO[1985]).

\*LIMS-derived NO<sub>y</sub> in parts per billion by volume (ppbv).

†Monthly average NO<sub>y</sub> (ppbv) from the case 1 simulation obtained by interpolating data from 38 and 65 mbar model levels.

HNO<sub>3</sub> by precipitation becomes important below 315 mbar, complemented by the faster rate of dry removal of HNO<sub>3</sub> at the surface, leading to comparable abundances of NO<sub>x</sub> and HNO<sub>3</sub> near the surface in the summer hemisphere. NO<sub>x</sub> surface mixing ratios in the extratropics exhibit a significant seasonal maximum in winter because OH levels are much lower during this period.

#### 4.2. Comparisons of Zonal Average NO<sub>y</sub> Fields From the Case 1 and Case 2 Experiments

The previous section has highlighted the fact that in the model the stratospheric source appears to have only a minimal impact on lower tropospheric NO<sub>y</sub> mixing ratios. A large fraction of the NO<sub>y</sub> transported down from the stratosphere is in the form of HNO<sub>3</sub>. The fraction of NO<sub>y</sub> injected into the troposphere in the form of NO<sub>x</sub> is converted relatively rapidly to HNO<sub>3</sub>, which is removed quite efficiently by wet and dry sinks in the lower troposphere. There has been some speculation that formation of relatively long-lived organic nitrogen species (such as PAN) from NO<sub>x</sub> could serve to increase the overall lifetime of NO<sub>y</sub> in the troposphere. According to this argument the organic species serve as temporary reservoirs for active nitrogen. For example, this mechanism, applied to fossil fuel combustion emissions, has been used in an attempt to explain NO<sub>x</sub> and O<sub>3</sub> mixing ratios observed in the high latitude troposphere over North America and Greenland during the Atmospheric Boundary Layer Experiment 3A (ABLE 3A) [Singh *et al.*, 1991a, 1991b].

In this section we focus on the question of whether the sequestering of NO<sub>x</sub> into temporary organic reservoirs might affect model-calculated tropospheric NO<sub>y</sub> mixing ratios and attempt to assess the magnitude of this effect. We feel that the design of the case 2 experiment provides a realistic upper limit of the impact of tropospheric production of organic nitrogen species on NO<sub>y</sub> distributions resulting from the stratospheric source (refer to the discussion in section 3).

Figure 5 illustrates the differences in NO<sub>y</sub> fields between the case 2 and case 1 simulations. Inclusion of PAN chemistry in the model does not alter simulated NO<sub>y</sub> levels by more than 10% above 500 mbar since the wet sink is relatively weak above this level. The case 2 simulation yields enhanced NO<sub>y</sub> mixing ratios, usually by factors of 1.3–4, in the middle and high latitude lower troposphere. The magnitude of the effect is generally larger in the northern hemi-

ACCEPTED MANUSCRIPT

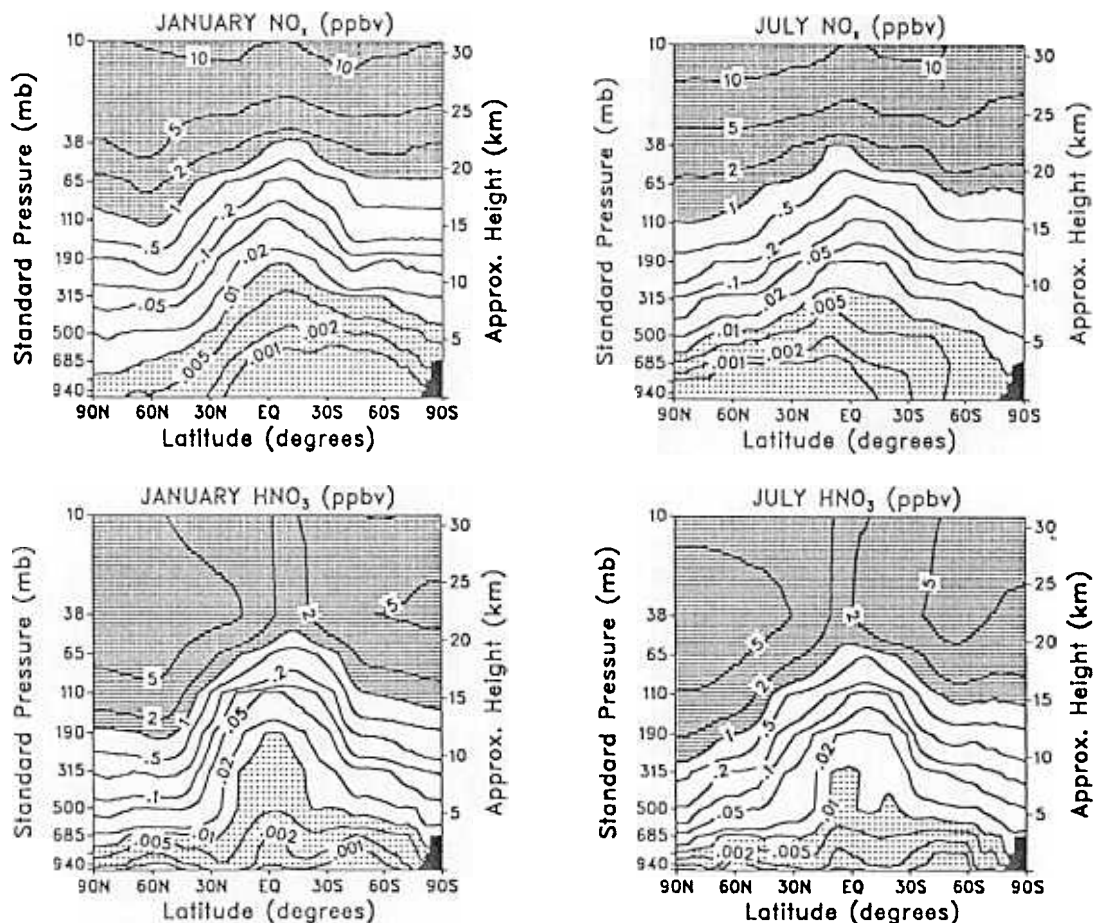


Fig. 4. Monthly average, zonal mean mixing ratios (ppbv) of  $\text{NO}_x$  and  $\text{HNO}_3$  from the case 1 experiment for the indicated months. Contour levels are logarithmic.

sphere, except during the northern winter. This is a direct consequence of higher PAN production rates in the northern hemisphere which is a result of the interhemispheric difference in hydrocarbon concentrations. In spite of the extreme sensitivity of the rate of PAN decomposition to temperature the model results show the counterintuitive feature that PAN formation has a smaller effect on lower tropospheric  $\text{NO}_y$  levels at higher latitudes in winter. This is because photochemical activity (and therefore conversion of  $\text{NO}_x$  to  $\text{HNO}_3$  as well as PAN formation in the upper troposphere) is greatly suppressed in winter at high latitudes. Inclusion of the PAN reactions also has a relatively minor effect (10–20%) on tropical surface  $\text{NO}_y$  mixing ratios owing to the rapid rate of thermal decomposition of PAN.

These differences in total  $\text{NO}_y$  fields between the two experiments can be related to the corresponding changes in  $\text{NO}_x$  and  $\text{HNO}_3$  fields (Figure 6). We will illustrate our discussions with model results from January and July. In the following discussion we shall use the terms “suppressed” and “enhanced” to refer to changes relative to the case 1 experiment, i.e., relative to the simulation with no PAN chemistry. Net photochemical production of PAN has the effect of suppressing  $\text{NO}_x$  mixing ratios in the middle and upper troposphere. During January the largest effect on  $\text{NO}_x$  occurs in a relatively small region centered around 500 mbar in the northern tropics and also in the midtroposphere of the high latitude southern hemisphere. Thermal decomposition

of PAN subsequently serves as a source of  $\text{NO}_x$  (some of which is converted to  $\text{HNO}_3$ ) in the lower troposphere, leading to enhanced levels of  $\text{NO}_x$  and, to a lesser extent, of  $\text{HNO}_3$  near the surface. A similar picture unfolds in July, though on a larger spatial scale.  $\text{NO}_x$  mixing ratios are suppressed by at least 10% over most of the northern hemisphere between 315 and 500 mbar.  $\text{HNO}_3$  levels in this region are also suppressed, since some of the  $\text{NO}_x$  which would otherwise be converted to  $\text{HNO}_3$  is now sequestered in the form of PAN. PAN decomposition leads to enhanced  $\text{NO}_x$  mixing ratios in the lower troposphere, by factors of 2–5, over a broad region extending poleward from 30°N, with corresponding  $\text{HNO}_3$  mixing ratios enhanced by 10–50%. Inclusion of PAN chemistry has a greater impact on northern hemisphere model results due to the aforementioned interhemispheric difference in hydrocarbon mixing ratios. This fact is also illustrated in model-simulated PAN distributions (see Figure 7). During the southern summer the highest PAN mixing ratios are of the order of 2–5 pptv. By contrast, model-simulated PAN mixing ratios range from 10–20 pptv in the middle and upper troposphere of the extratropical northern hemisphere during July. The rapid rate of thermal decomposition of PAN results in extremely low PAN mixing ratios in the tropical lower troposphere. This result is consistent with measurements by Rudolph and Muller [1990] in the remote South Atlantic, where surface PAN levels were typically below 0.5 pptv.

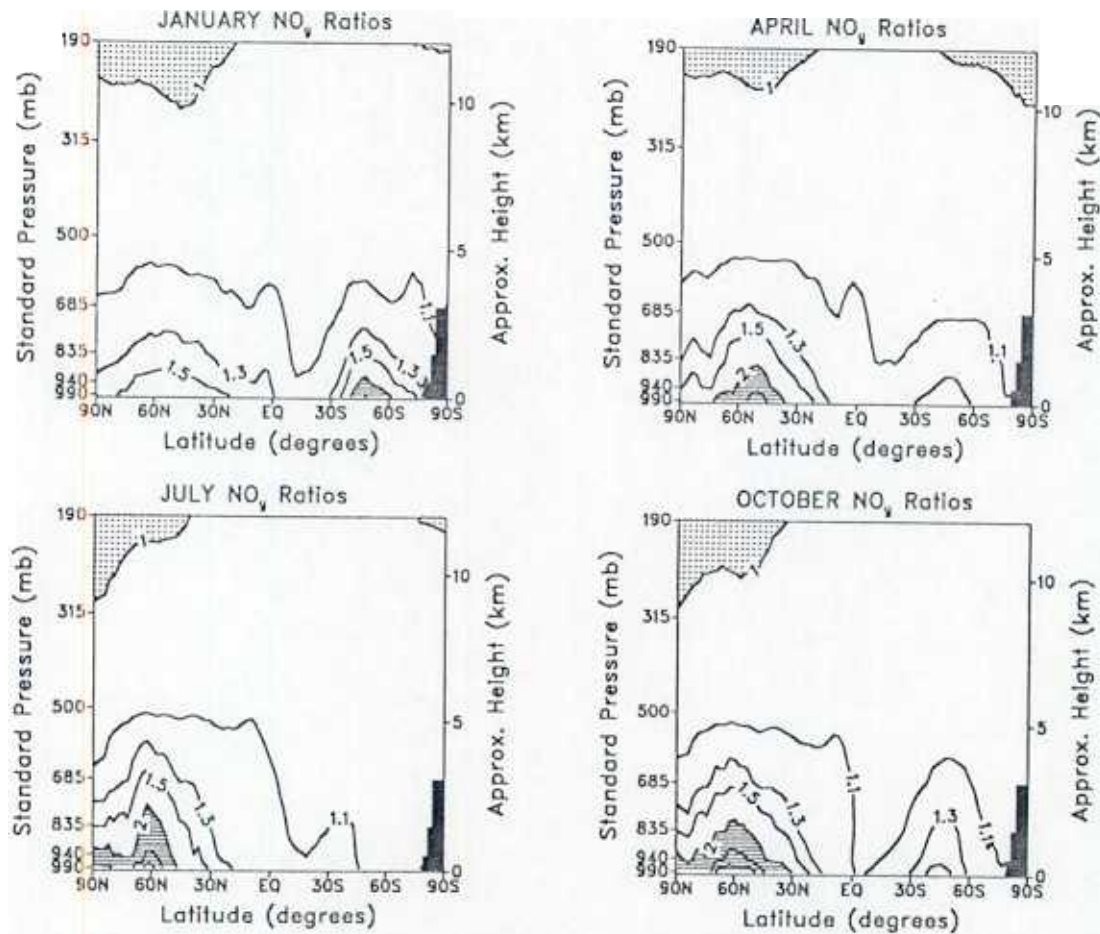


Fig. 5. Ratio of model-calculated NO<sub>y</sub> mixing ratios with PAN chemistry (case 2 experiment) to mixing ratios obtained without including PAN chemistry (case 1 experiment). Lightly shaded areas represent regions where case 2 results are less than or equal to case 1 results, while heavily shaded areas represent regions where case 2 results are at least a factor of 2 higher than case 1 results. Contour levels are 1, 1.1, 1.3, 1.5, 2, 3, and 4.

Our results therefore suggest that sequestering of active nitrogen into relatively long-lived, temporary reservoirs (such as PAN) could be important, especially in the middle and higher latitudes of the northern hemisphere lower troposphere where neglecting this effect may cause NO<sub>x</sub> levels to be underpredicted by factors of 1.5 to >5. Such a mechanism could presumably be equally significant for other NO<sub>y</sub> sources and especially for the upper tropospheric lightning source. We caution, however, that these results should be interpreted with some care since the chemistry involved is quite complex and not yet fully understood. The results from the case 2 experiment should therefore be viewed in the context of providing an upper limit to our calculations of the tropospheric impact of the stratospheric NO<sub>y</sub> source, while the case 1 results provide the corresponding lower limit.

#### 4.3. Surface Mixing Ratios

One of the main thrusts of this study is to examine the impact of stratospheric production on surface NO<sub>y</sub> mixing ratios. As mentioned earlier, a previous study by Levy and Moxim [1989] found that emissions from fossil fuel combustion could account for less than 10% of observed surface NO<sub>y</sub> in regions remote from the predominantly northern hemisphere, mid-latitude source regions. On the basis of

results scaled from a stratified tracer experiment [Mahlman *et al.*, 1980], Levy *et al.* [1980] hypothesized that stratospheric production of NO could be a significant source of NO<sub>y</sub> for the remote troposphere, accounting for up to half the observed NO<sub>y</sub> in these regions. Their model-calculated, surface mixing ratios were in reasonable agreement with the lowest NO<sub>y</sub> concentrations measured over the equatorial Pacific [Huebert, 1980]. Levy and Moxim [1989] also used the fact that seasonal cycles of surface O<sub>3</sub> [Oltmans, 1981] and surface aerosol nitrate [Savoie *et al.*, 1989] at Samoa were similar, as an argument in favor of an upper tropospheric or stratospheric source of NO<sub>y</sub> in the remote troposphere. However, calculations by Savoie *et al.* [1989] revealed that there was almost no correlation between measured surface <sup>7</sup>Be and aerosol nitrate and between surface O<sub>3</sub> and aerosol nitrate, and they concluded that the stratosphere has a minimal impact on tropospheric NO<sub>y</sub>.

In this section we readdress some of these issues by comparing model simulations of surface NO<sub>y</sub> with earlier estimates by Levy *et al.* [1980]. The major differences between the two studies are the explicitly calculated NO<sub>y</sub> source distribution, the partitioning of NO<sub>y</sub> into NO<sub>x</sub>, HNO<sub>3</sub>, and PAN (in the case 2 experiment) in the current study and in the wet removal parameterization used. We will also present some comparisons of our results with an esti-

ACCEPTED MANUSCRIPT

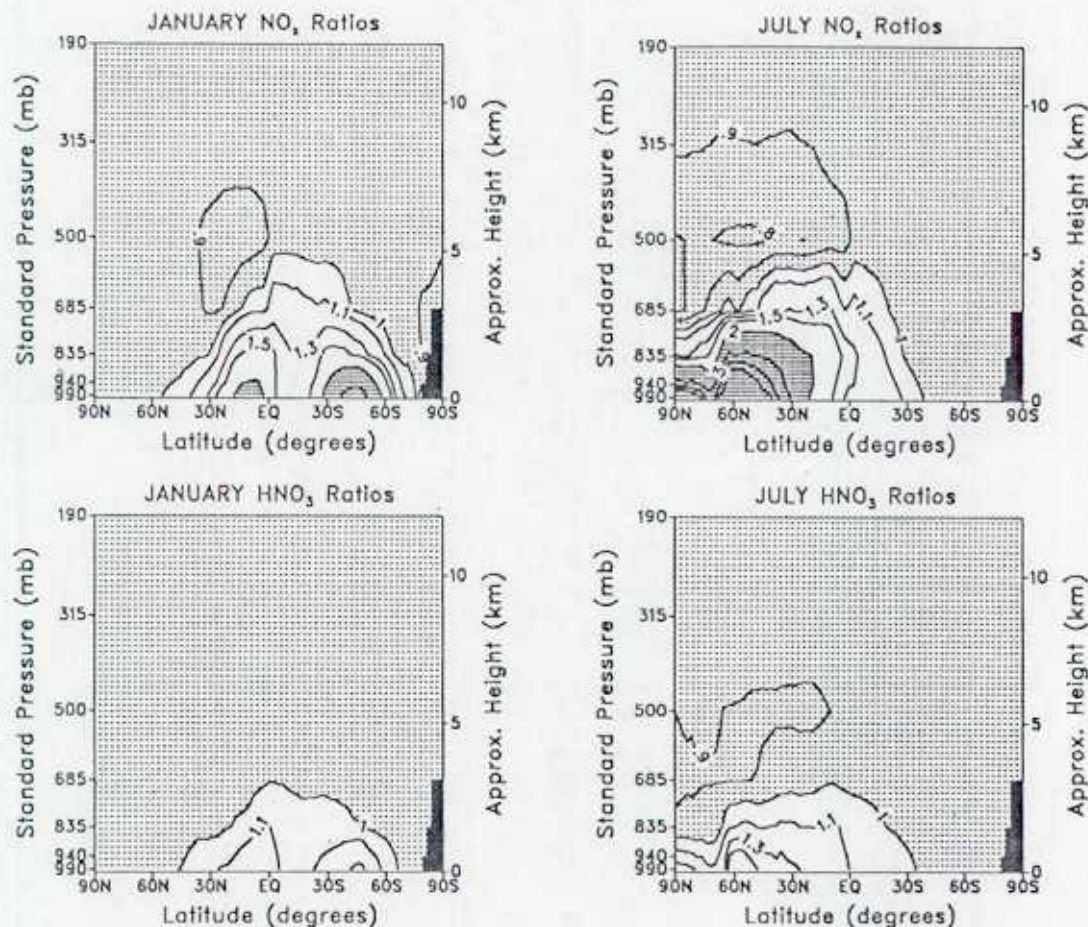


Fig. 6. Ratio of model-calculated  $\text{NO}_x$  and  $\text{HNO}_3$  mixing ratios from case 2 experiment to mixing ratios from the case 1 experiment. Lightly shaded areas represent regions where case 2 results are less than or equal to case 1 results, while heavily shaded areas represent regions where case 2 results are at least a factor of 2 higher than case 1 results. Contour levels are 0.8, 0.9, 1, 1.1, 1.3, 1.5, 2, 3, 4, and 5.

mate by Levy and Moxim [1989] of surface  $\text{NO}_y$  distributions resulting from fossil fuel combustion emissions alone, in an attempt to identify regions where the small stratospheric source could be of importance. We emphasize, however, that such an evaluation is preliminary since the fossil fuel combustion experiment by Levy and Moxim [1989] differs in terms of the number of transported species and the wet removal scheme used in the model. We will use the results from the case 2 experiment in our discussions below to provide an estimate of the upper limit of the impact of the stratospheric source.

The annually averaged, surface  $\text{NO}_y$  mixing ratio fields from the case 2 experiment is presented in Figure 8. Lowest surface  $\text{NO}_y$  mixing ratios are found in the model tropics, while highest levels are found poleward of  $60^\circ$ . The model-simulated mixing ratios range from 2–5 pptv in mid-latitudes and from 5–10 pptv in the polar regions. These are extremely low mixing ratios and are about a factor of 5 to 10 lower than those obtained by Levy *et al.* [1980]. Surface  $\text{NO}_y$  mixing ratios from the case 2 experiment may also be compared with model calculations of corresponding fields produced by fossil fuel combustion emissions alone (see Figure 3, Levy and Moxim [1989]). As expected, downward transport from the stratosphere is relatively insignificant over the continental fossil fuel combustion source regions and over the

northern hemisphere mid-latitude oceans downwind of these source regions. Our model results also indicate that the stratospheric source may have a greater impact on surface  $\text{NO}_y$  than the fossil fuel source in the middle and high latitude southern hemisphere away from fossil fuel combustion regions.

A more detailed comparison of model-calculated, annually averaged surface mixing ratios with multiple-year observations from the Sea-Air Exchange (SEAREX) network [Prospero and Savoie, 1989] is shown in Table 2. While emissions from fossil fuel combustion explain 40–50% of observed nitrate levels in the North Pacific (assuming most of the model  $\text{NO}_y$  from the fossil fuel source is in the form of  $\text{HNO}_3$  at these remote locations), transport from the stratosphere usually accounts for less than 2% of observed nitrate at these sites. Discrepancies between model simulations and observations in the tropical South Pacific, where less than 10% of observed nitrate can be accounted for by fossil fuel combustion and stratospheric injection, suggest an important role for other sources such as biomass burning,  $\text{NO}_x$  production by lightning discharges, or biogenic emissions associated with soil microbial activity. We once again caution, however, that this conclusion is preliminary, at least in a quantitative sense, since the fossil fuel simulation has not

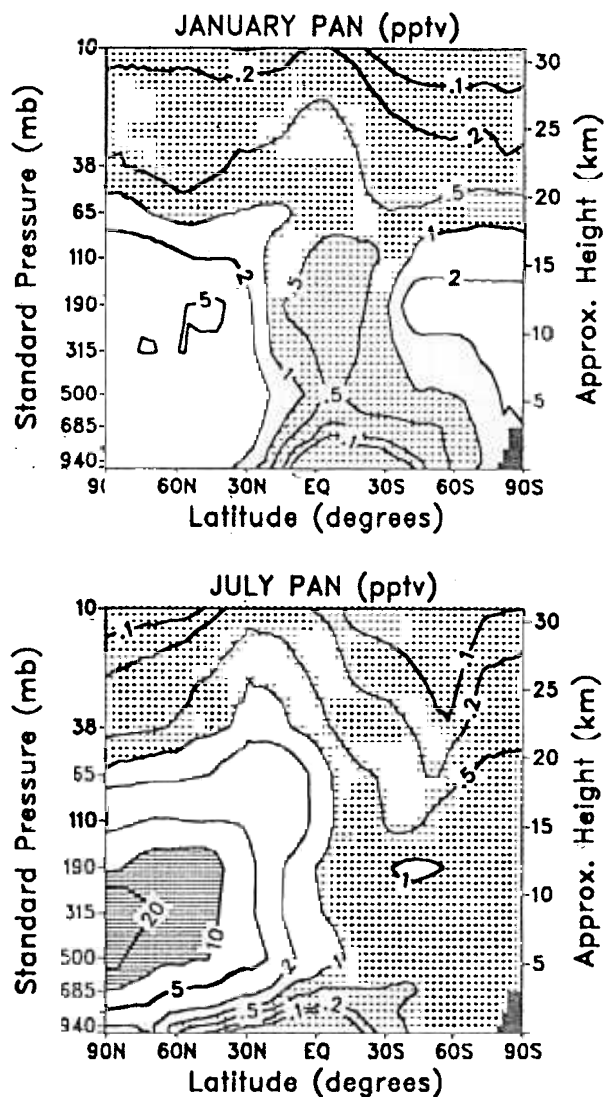


Fig. 7. Monthly average, zonal mean PAN mixing ratios from the case 2 experiment for the indicated months. Contour levels are logarithmic.

yet been exercised with the current chemical and wet removal schemes.

It is also instructive to compare model surface PAN mixing ratios with some recent measurements at high northern latitudes during the ABLE 3A experiment [Singh *et al.*, 1991a]. The median PAN level in the 0–2 km altitude range during July was of the order of 25 pptv (see Figure 2, Singh *et al.* [1991a]). Our July mean PAN mixing ratios from the case 2 experiment are less than 2 pptv between the surface and the 835 mbar model level, between 60° and 70°N over Alaska. It thus seems unlikely that the stratospheric source is an important factor in determining the tropospheric NO<sub>y</sub> budget of this region.

An analysis of deposition fields from the experiment also reveals that stratospheric injection has a negligible impact on observed deposition rates at remote locations, as previously argued by Logan [1983]. Observed NO<sub>y</sub> deposition rates at these locations range from 2–4 m mols N m<sup>-2</sup> yr<sup>-1</sup>, while deposition rates due to the stratospheric source are generally less than 0.1 m mols N m<sup>-2</sup> yr<sup>-1</sup>.

#### 4.4. Middle and Upper Troposphere Mixing Ratios

The previous section demonstrated that the stratospheric source appears to have a negligible impact on lower tropospheric NO<sub>y</sub> concentrations, both in the remote tropics and at high latitudes. We now turn our attention to the middle and upper troposphere. Consider the model-derived, annually averaged, 500 mbar mixing ratio fields from the case 2 experiment (Figure 9). This plot may be compared with the corresponding map from Levy and Moxim [1989] for a simulation with the fossil fuel combustion source alone. In the tropics the two sources yield comparable NO<sub>y</sub> mixing ratios, ranging from 5 to 20 pptv. Mixing ratios from combustion emissions range from 50 pptv to greater than 100 pptv in the northern mid-latitudes, with the larger values occurring at and downwind of the major source regions in North America, Europe, and Asia. The corresponding mixing ratios from the case 2 experiment are of the order of 20–50 pptv south of about 40°N and 50–100 pptv at higher latitudes. In the southern hemisphere midtroposphere, NO<sub>y</sub> mixing ratios from the fossil fuel source range from 10 to 20 pptv near continental source regions, with smaller values (<5 pptv) occurring in more remote locations. This is because very little NO<sub>y</sub> from the northern hemisphere combustion emissions is transported to the southern hemisphere due to efficient removal at the ITCZ. Model-simulated NO<sub>y</sub> mixing ratios from the stratospheric source range from 10–20 pptv in the southern hemisphere mid-latitudes and from 20–50 pptv poleward of 60°S, indicating that the stratospheric source is at least as, if not more, important than the fossil fuel source over much of the southern hemisphere midtroposphere. Higher up in the troposphere, at the 315 mbar model level, NO<sub>y</sub> mixing ratios from the stratospheric source are about a factor of 2 higher than those produced by the fossil fuel source during summer in the northern hemisphere mid-latitudes. However, the stratospheric source dominates during winter/spring in the northern hemisphere since this is the period of strongest downward transport from the stratosphere and also due to the fact that convective upward transport of fossil fuel NO<sub>y</sub> is at a minimum during this period.

The available observational data on total NO<sub>y</sub> in the middle and upper troposphere consists of relatively short term measurements, confined to a few specific locations. It is instructive, however, to compare model results with these observations. NO<sub>y</sub> measurements over one southern hemisphere station (Darwin, Australia; 12°S, 131°E) and two northern hemisphere stations (Guam, 14°N, 145°E and Hickam Air Force Base, Hawaii, 21°N, 158°W) were conducted as part of the Stratosphere-Troposphere Exchange Program (STEP) during January and February 1987. Our model calculations yield January average mixing ratios in the range of 10 to 50 pptv in the vicinity of Darwin and Guam at the 190 and 315 mbar model levels, while the average observed mixing ratio is approximately 400 pptv (D. M. Murphy *et al.*, Reactive odd nitrogen and its correlation with ozone in the lower stratosphere and upper troposphere, submitted to *Journal of Geophysical Research*, 1991). Similarly, at Hawaii, model-calculated values (20–100 pptv) differ substantially from the observations (250–600 pptv). Estimates of NO<sub>y</sub> levels from the fossil fuel combustion source [Levy and Moxim, 1989] are insufficient to account for more than a small fraction of these measurements. This

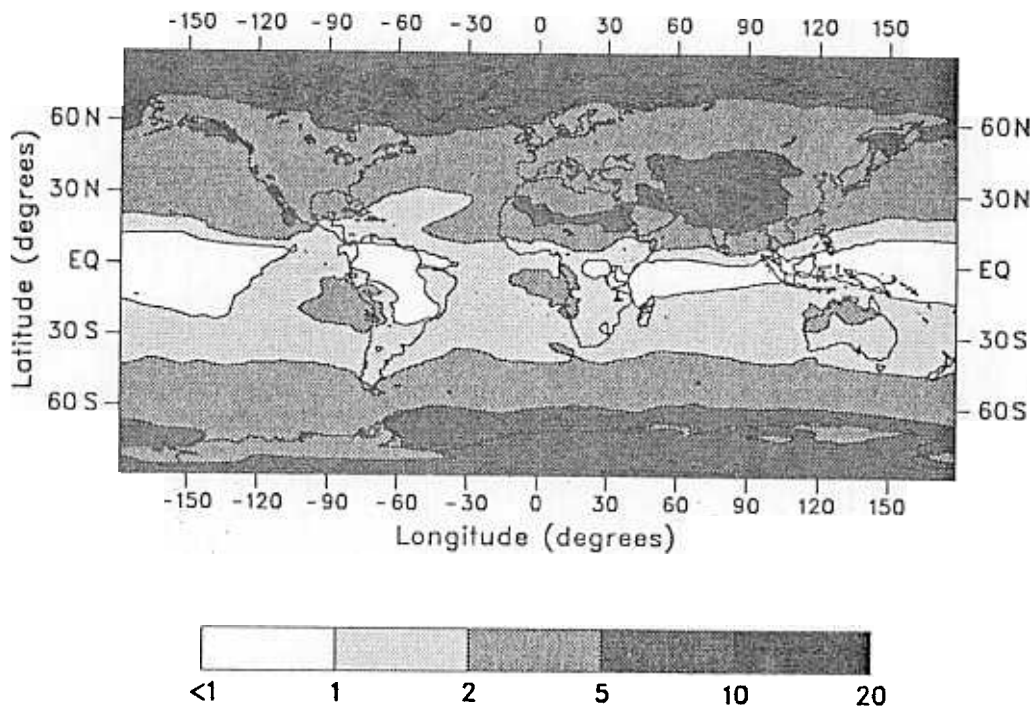


Fig. 8. Annually averaged surface NO<sub>y</sub> mixing ratios (pptv) from the case 2 experiment. Contour levels logarithmic.

large discrepancy between observations and model calculations points to an important role for other NO<sub>y</sub> sources such as biomass burning and production of NO<sub>x</sub> by lightning discharges. While the biomass burning source could account for at least part of the deficit in the northern tropics, it cannot explain the large deficit at the southern hemisphere site, especially since the particular time period does not correspond to the burning season in the southern tropics. Taking into account the fact that the measurement period corresponds to the southern hemisphere lightning season [Orville and Henderson, 1986], it seems plausible that NO<sub>x</sub> production by lightning discharges (as suggested by D. M. Murphy et al., 1991) could be the dominant source of NO<sub>y</sub> in the southern tropics during this period.

An additional set of NO<sub>y</sub> measurements in the middle troposphere are those performed as part of the NASA Global Tropospheric Experiment/Chemical Instrumentation Test and Evaluation 2 (GTE/CITE 2) experiment during August and September 1986, over the eastern North Pacific between 30° and 45°N. Values ranging from ~150 pptv to greater than 800 pptv, with a mean of ~300 pptv, were observed at altitudes of 4.5–6 km [Ridley et al., 1990]. Our model simulations yield mixing ratios ranging from 20 to 50 pptv at the 500 mbar model level from the stratospheric source, which leads us to the conclusion that the NO<sub>y</sub> mixing ratios over this region of the North Pacific are not strongly influenced by the stratospheric source. Calculations by Levy and Moxim [1989] suggest that export of fossil fuel combustion

TABLE 2. Comparison of Case 2 Model Results With SEAREX Surface Observations

Station	Observation*	Combustion†	Stratosphere‡			
			NO <sub>x</sub>	HNO <sub>3</sub>	PAN	NO <sub>y</sub>
Shemya, 53°N, 174°E	94	74				
Midway, 28°N, 177°W	104	62				
Oahu, 21°N, 158°W	130	49				
Enewetak, 11°N, 162°E	56	25	<1			
Fanning, 4°N, 159°W	59	16	<1			
Nauru, 1°S, 167°E	59	7	<1			
Funafuti, 8°S, 179°E	39	6	<1			
Samoa, 14°S, 171°W	40	6	<1			1
Rarotonga, 21°S, 160°W	42	6	<1			1
New Caledonia, 22°S, 166°E	76	55				2
Norfolk Island, 29°S, 169°E	66	30				2

Observations are soluble reactive nitrogen measurements, while model results are at the 990 mbar model level. All values are in parts per trillion by volume.

\*Soluble reactive nitrogen measurements from Prospero and Savoie [1989].

†Model NO<sub>y</sub> with the fossil fuel combustion source alone from Levy and Moxim [1989].

‡Model results from the case 2 experiment.

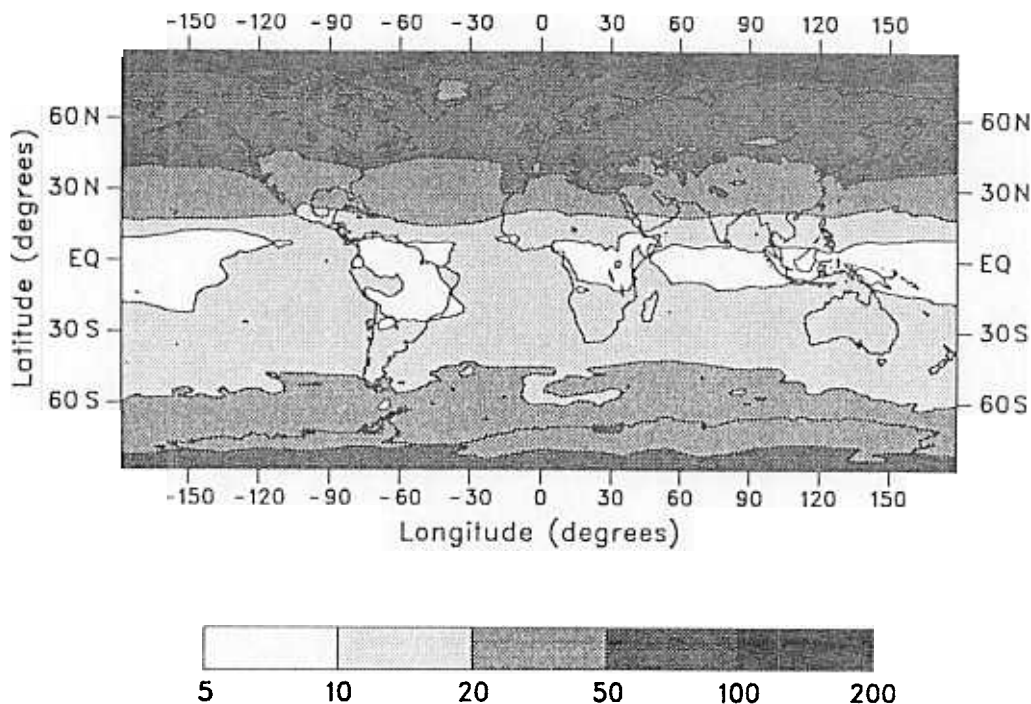


Fig. 9. Annually averaged 500 mbar NO<sub>y</sub> mixing ratios (pptv) from the case 2 experiment. Contour levels are logarithmic.

emissions from continental source regions results in NO<sub>y</sub> mixing ratios ranging from 50 to 200 pptv over this region during the summer. Once again, emissions associated with biomass burning in Asia and NO<sub>x</sub> production by lightning may account for the remaining part of the NO<sub>y</sub>. However, the relative importance of these two sources in this region remains to be quantified.

It is also interesting to note that July mean PAN mixing ratios from the case 2 simulation range from 10 to 20 pptv between the 315 and 500 mbar model levels, over Alaska between 60° and 70°N. These values may be compared with the observed median PAN mixing ratio of ~270 pptv during the ABLE 3A experiment [Singh *et al.*, 1991] at an altitude range of 4–6 km, again suggesting that the stratospheric source is a minor contributor to the tropospheric NO<sub>y</sub> budget at high latitudes.

#### SUMMARY

In this study we have reevaluated the hypothesis that downward transport of NO<sub>y</sub> produced in the stratosphere might explain as much as half the observed surface NO<sub>y</sub> in the remote troposphere. Using specified, zonally averaged O<sub>3</sub> and N<sub>2</sub>O fields, along with monthly averaged pressure and temperature fields from the GFDL SKYHI GCM, we have calculated a temporally varying, two-dimensional NO source function for input into a GCTM. Our model simulations, with a partitioning of NO<sub>y</sub> into NO<sub>x</sub>, HNO<sub>3</sub>, and PAN, suggest that earlier estimates of surface NO<sub>y</sub> concentrations, resulting from downward transport of NO<sub>x</sub> produced in the stratosphere, may be overestimated by a factor of 5 to 10. Our current study also indicates that model calculations which do not incorporate PAN chemistry may significantly underpredict NO<sub>x</sub> and NO<sub>y</sub> concentrations in the lower troposphere. A more realistic treatment of the

chemistry of long-lived organics in global transport models is clearly an area which warrants further investigation, as it could have major implications for our understanding of NO<sub>y</sub> distributions from other sources as well.

The model results, in conjunction with an earlier assessment of NO<sub>y</sub> distributions from fossil fuel combustion emissions, imply a major role for other possible sources of surface NO<sub>y</sub> in the remote tropics and in the southern hemisphere. Comparisons of model-calculated midtropospheric background NO<sub>y</sub> mixing ratios with observations in the tropics and subtropics also suggest that biomass burning and nitrogen fixation associated with lightning discharges may contribute significantly to the tropospheric NO<sub>y</sub> budget. Uncertainties associated with source strengths, transport, chemistry, and removal still persist. However, we feel that our two principal conclusions regarding the minimal impact of the stratospheric source on remote lower tropospheric NO<sub>y</sub> mixing ratios and the need for a significant source of NO<sub>y</sub> in the tropical middle and upper troposphere are valid.

#### APPENDIX: PARTITIONING OF NO<sub>y</sub> INTO SOLUBLE AND INSOLUBLE SPECIES

An accurate determination of the fraction of the individual nitrogen species that make up NO<sub>y</sub> requires the solution of a coupled set of stiff partial differential equations. Since solution methods for these types of systems are extremely time consuming, various simplifying assumptions are often made to obtain approximate solutions to this problem. We describe below a simplified chemical scheme, which enables us to explicitly calculate the partitioning of NO<sub>y</sub> into soluble and insoluble fractions, without resorting to iterative solution schemes. Chemical production and loss rates of the soluble and insoluble fractions are calculated based on the reaction of NO<sub>2</sub> and HNO<sub>3</sub> with OH and the photodissoci-

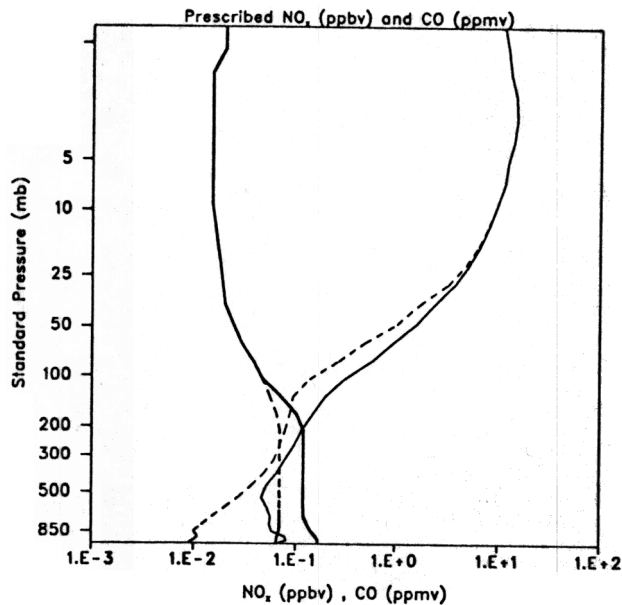
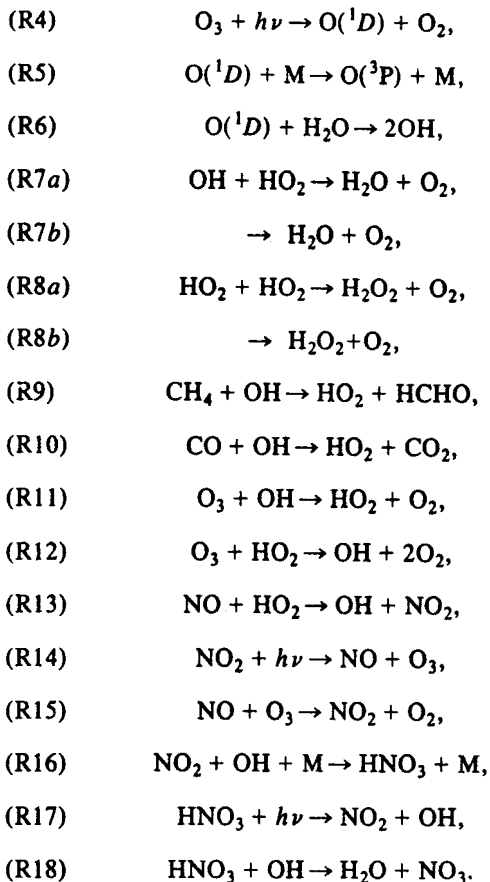


Fig. 10. Prescribed one-dimensional NO<sub>x</sub> (light lines) and CO (heavy lines) vertical profiles used in the calculation of tropospheric OH fields. Solid lines represent northern hemisphere profiles, while dashed lines represent southern hemisphere profiles.

ation of HNO<sub>3</sub>. The essence of the method involves capturing the spatial variation of the OH concentration field and scaling these concentrations so as to yield a tropospheric methyl chloroform lifetime of 6.2 years [Prinn *et al.*, 1987]. The set of chemical reactions considered are



Using recent estimates of kinetic parameters [DeMore *et al.*, 1990], specified one-dimensional NO<sub>x</sub> and CO profiles in each hemisphere (Figure 10); specified two-dimensional O<sub>3</sub> (see Figure 1) and CH<sub>4</sub> fields (Figure 11), and monthly average temperature, pressure, and water vapor fields from the GFDL SKYHI GCM [Hamilton and Mahlman, 1988], from (R4) and (R5) we calculate zonally averaged O(<sup>1</sup>D) concentrations as

$$n(O^1D) = \frac{J_1 n(O_3)}{k_2 n(M)}, \quad (6)$$

where the  $n$  coefficient represents number density,  $J_i$  is the photolysis rate coefficient for reaction  $i$ , and  $k_j$  is the specific reaction rate for reaction  $j$ . The NO/NO<sub>2</sub> ratio is calculated from (R14) and (R15) based on the assumption of a photo-stationary state among NO, NO<sub>2</sub>, and O<sub>3</sub> as

$$\frac{n(NO)}{n(NO_2)} = \frac{J_{11}}{k_{12} n(O_3)}, \quad (7)$$

and NO and NO<sub>2</sub> concentrations are calculated using the specified NO<sub>x</sub> concentrations.

From (R9) to (R13) and assuming that the HO<sub>2</sub>-OH cycling reactions are relatively rapid enables us to write

$$\text{RATIO} = \frac{n(HO_2)}{n(OH)} = \frac{k_6 n(CH_4) + k_7 n(CO) + k_8 n(O_3)}{k_9 n(O_3) + k_{10} n(NO)}. \quad (8)$$

On the basis of a balance between radical production and destruction (reactions (R6), (R7a), (R7b), (R8a), and (R8b)) and using the HO<sub>2</sub>/OH ratio calculated from (6), we calculate the OH concentration as

$$n(OH) = \left[ \frac{k_3 n(O^1D) n(H_2O)}{k_4 (\text{RATIO}) + k_5 (\text{RATIO})^2} \right]^{1/2} \times \text{FACT}, \quad (9)$$

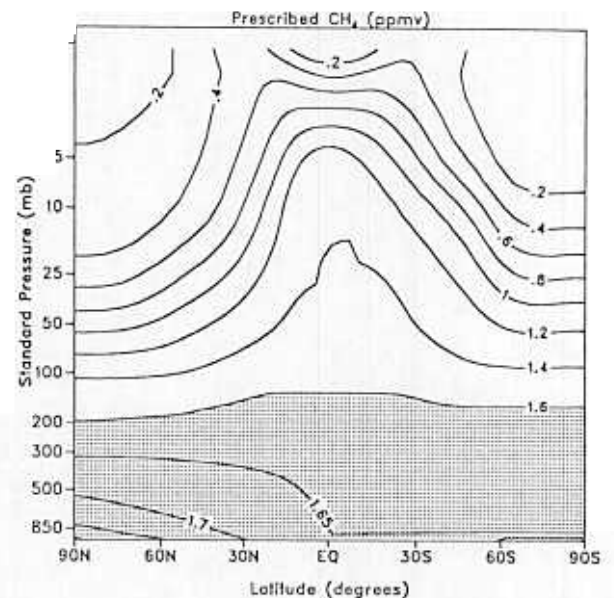


Fig. 11. Prescribed CH<sub>4</sub> field (ppmv) used in the calculation of tropospheric OH fields. Contour levels are 0.2, 0.4, 0.6, 0.8, 1.0, 1.2, 1.4, 1.6, 1.65, 1.7, and 1.75 ppmv.

where FACT is an empirically determined correction factor. This correction factor is determined by scaling the OH fields to yield a globally and annually averaged methyl chloroform lifetime of 6.2 years [Prinn et al., 1987]. Specifically, we obtain FACT  $\approx$  2 and a scaled globally and annually averaged tropospheric OH concentration of  $6.7 \times 10^5$  molecules cm<sup>-3</sup>. The large value of the correction factor is due to the simplifying assumptions made to facilitate the OH calculation. The zonally averaged, scaled tropospheric OH fields calculated in this manner compare reasonably well with tropospheric OH fields derived using a more detailed implicit chemical scheme based on a CH<sub>4</sub>-CO-NO<sub>x</sub>-O<sub>3</sub>-H<sub>x</sub>O<sub>y</sub> mechanism [e.g., Chameides and Tan, 1981; Spivakovsky et al., 1990]. The sharp gradients in the boundary layer near the equator are related to the very simple, hemispherically averaged, one-dimensional distribution assumed for NO<sub>y</sub>.

We then use these scaled OH fields to specify NO<sub>x</sub>/HNO<sub>3</sub> production and destruction rates in the form of lookup tables to the transport model. While the simple chemical scheme clearly has limitations, especially in its treatment of the radical cycling reactions, these are not of great significance in this study since a large fraction of the NO<sub>y</sub> transported to the troposphere from the stratosphere is in the form of HNO<sub>3</sub>, and this feature is captured with the simple chemical scheme.

*Acknowledgments.* This work was supported in part by funds from the National Science Foundation under grant ATM-8701289. We wish to thank D. W. Fahey, K. Hamilton, J. D. Mahlman, D. M. Murphy, and S. E. Strahan for their perceptive comments on the original manuscript. We are especially grateful to S. C. Liu and an anonymous reviewer for their thoughtful comments and suggestions. We also wish to express our gratitude to D. M. Murphy and D. W. Fahey for providing unpublished data.

#### REFERENCES

- Atkinson, R., and A. C. Lloyd, Evaluation of kinetic and mechanistic data for modeling of photochemical smog, *J. Phys. Chem. Ref. Data*, **13**, 315-440, 1984.
- Cadle, S. H., J. M. Dasch, and P. A. Mulawa, Atmospheric concentrations and the deposition velocity to snow of nitric acid, sulfur dioxide and various particulate species, *Atmos. Environ.*, **19**, 1819-1827, 1985.
- Chameides, W. L., and A. Tan, The two-dimensional diagnostic model for tropospheric OH: An uncertainty analysis, *J. Geophys. Res.*, **86**, 5209-5223, 1981.
- Crutzen, P. J., Photochemical reaction initiated by and influencing ozone in unpolluted tropospheric air, *Tellus*, **26**, 45-55, 1974.
- Crutzen, P. J., and U. Schmailzl, Chemical budgets of the stratosphere, *Planet. Space Sci.*, **31**, 1009-1020, 1983.
- DeMore, W. B., J. J. Margitan, M. J. Molina, R. T. Watson, D. M. Golden, R. F. Hampson, M. J. Kurylo, C. J. Howard, and A. R. Ravishankara, Chemical kinetics and photochemical data for use in stratospheric modeling, Evaluation number 9, NASA, *JPL Publ. 90-1*, 217 pp., Pasadena, Calif., 1990.
- Giorgi, F., and W. L. Chameides, Rainout lifetimes of highly soluble aerosols and gases as inferred from simulations with a general circulation model, *J. Geophys. Res.*, **91**, 14,367-14,376, 1986.
- Hamilton, K., and J. D. Mahlman, General circulation model simulation of the semiannual oscillation of the tropical middle atmosphere, *J. Atmos. Sci.*, **45**, 3214-3235, 1988.
- Huebert, B. J., Nitric acid and aerosol nitrate measurements in the equatorial Pacific region, *Geophys. Res. Lett.*, **7**, 325-328, 1980.
- Huebert, B. J., and C. H. Robert, The dry deposition of nitric acid to grass, *J. Geophys. Res.*, **90**, 2085-2090, 1985.
- Jackman, C. H., J. E. Frederick, and R. S. Stolarski, Production of odd nitrogen in the stratosphere and mesosphere: An intercomparison of source strengths, *J. Geophys. Res.*, **85**, 7495-7505, 1980.
- Kley, D., J. W. Drummond, M. McFarland, and S. C. Liu, Tropospheric profiles of NO<sub>x</sub>, *J. Geophys. Res.*, **86**, 3153-3161, 1981.
- Legrand, M. R., F. Stordal, I. S. A. Isaksen, and B. Rognerud, A model study of the stratospheric budget of odd nitrogen including effects of solar cycle variations, *Tellus*, **41**, 413-426, 1989.
- Leighton, P. A., *Photochemistry of Air Pollution*, 300 pp., Academic, San Diego, Calif., 1961.
- Levy, H., II, Normal atmosphere: Large radical and formaldehyde concentrations predicted, *Science*, **173**, 141-143, 1971.
- Levy, H., II, and W. J. Moxim, Simulated global distribution and deposition of reactive nitrogen emitted by fossil fuel combustion, *Tellus*, **41**, 256-271, 1989.
- Levy, H., II, J. D. Mahlman, and W. J. Moxim, A stratospheric source of reactive nitrogen in the unpolluted troposphere, *Geophys. Res. Lett.*, **7**, 441-444, 1980.
- Levy, H., II, J. D. Mahlman, and W. J. Moxim, Tropospheric N<sub>2</sub>O variability, *J. Geophys. Res.*, **87**, 3061-3080, 1982.
- Levy, H., II, J. D. Mahlman, W. J. Moxim, and S. C. Liu, Tropospheric ozone: The role of transport, *J. Geophys. Res.*, **90**, 3753-3772, 1985.
- Liu, S. C., D. Kley, M. McFarland, J. D. Mahlman, and H. Levy, II, On the origin of tropospheric ozone, *J. Geophys. Res.*, **85**, 7546-7552, 1980.
- Logan, J. A., Nitrogen oxides in the troposphere: Global and regional budgets, *J. Geophys. Res.*, **88**, 10,785-10,807, 1983.
- Madronich, S., and J. G. Calvert, Permutation reactions of organic peroxy radicals in the troposphere, *J. Geophys. Res.*, **95**, 5697-5716, 1990.
- Mahlman, J. D., and W. J. Moxim, Tracer simulation using a global general circulation model: Results from a midlatitude instantaneous source experiment, *J. Atmos. Sci.*, **35**, 1340-1374, 1978.
- Mahlman, J. D., H. Levy, II, and W. J. Moxim, Three-dimensional tracer structure and behavior as simulated in two ozone precursor experiments, *J. Atmos. Sci.*, **37**, 655-685, 1980.
- Mahlman, J. D., H. Levy, II, and W. J. Moxim, Three-dimensional simulations of stratospheric N<sub>2</sub>O: Predictions for other trace constituents, *J. Geophys. Res.*, **91**, 2687-2707, 1986.
- Manabe, S., and J. L. Holloway, Jr., The seasonal variation of the hydrologic cycle as simulated by a global model of the atmosphere, *J. Geophys. Res.*, **80**, 1617-1649, 1975.
- Manabe, S., and J. D. Mahlman, Simulation of seasonal and interhemispheric variations in the stratospheric circulation, *J. Atmos. Sci.*, **33**, 2185-2217, 1976.
- Manabe, S., D. G. Hahn, and J. L. Holloway, Jr., The seasonal variation of the tropical circulation as simulated by a global model of the atmosphere, *J. Atmos. Sci.*, **31**, 43-83, 1974.
- National Research Council (NRC), *Acid Deposition: Atmospheric Processes in Eastern North America, A Review of Current Scientific Understanding*, 375 pp., National Academy Press, Washington, D. C., 1983.
- Oltmans, S. J., Surface ozone measurements in clean air, *J. Geophys. Res.*, **86**, 1174-1180, 1981.
- Orville, R. E., and R. W. Henderson, Global distribution of mid-night lightning: September 1977 to August 1978, *Mon. Weather Rev.*, **114**, 2640-2653, 1986.
- Prinn, R., D. Cunnold, R. Rasmussen, P. Simmonds, F. Alyea, A. Crawford, P. Fraser, and P. Rosen, Atmospheric trends in methylchloroform and the global average for the hydroxyl radical, *Science*, **238**, 945-950, 1987.
- Prospero, J. M., and D. L. Savoie, Effect of continental sources on nitrate concentrations over the Pacific Ocean, *Nature*, **339**, 687-689, 1989.
- Ridley, B. A., et al., Ratios of peroxyacetyl nitrate to active nitrogen observed during flights over the eastern Pacific oceans and continental United States, *J. Geophys. Res.*, **95**, 10,179-10,192, 1990.
- Rudolph, J., Two-dimensional distribution of light hydrocarbons: Results from the STRATOZ III experiment, *J. Geophys. Res.*, **93**, 8367-8377, 1988.
- Rudolph, J., and K. P. Muller, The latitudinal distribution of peroxyacetyl nitrate (PAN) in the atmospheric boundary layer over the Atlantic, paper presented at the 7th International Symposium of the Commission on Atmospheric Chemistry and Global Pollution, Chamrousse, France, 1990.
- Ryther, J. H., and W. M. Dunstan, Nitrogen, phosphorus, and

- eutrophication in the coastal marine environment, *Science*, *171*, 1008–1113, 1971.
- Savoie, D. L., J. M. Prospero, J. T. Merrill, and M. Uematsu, Nitrate in the atmospheric boundary layer of the tropical South Pacific: Implications regarding sources and transport, *J. Atmos. Chem.*, *8*, 391–415, 1989.
- Singh, H. B., and P. B. Zimmerman, Atmospheric distributions and sources of nonmethane hydrocarbons, *Adv. Environ. Sci. Technol.*, in press, 1991.
- Singh, H. B., D. O'Hara, D. Herlth, J. D. Bradshaw, S. T. Sandholm, G. L. Gregory, G. W. Sachse, D. R. Blake, P. J. Crutzen, and M. A. Kanakidou, Atmospheric measurements of PAN and other organic nitrates at high latitudes: Possible sources and sinks, *J. Geophys. Res.*, in press, 1991a.
- Singh, H. B., D. Herlth, D. O'Hara, K. Zahnle, J. D. Bradshaw, S. T. Sandholm, R. Talbot, P. J. Crutzen, and M. A. Kanakidou, Relationship of PAN to active and total odd nitrogen at northern high latitudes: Influence of reservoir species on NO<sub>x</sub> and O<sub>3</sub>, *J. Geophys. Res.*, in press, 1991b.
- Spivakovsky, C. M., R. Yevich, J. A. Logan, S. C. Wofsy, M. B. McElroy, and M. J. Prather, Tropospheric OH in a three-dimensional chemical tracer model: An assessment based on observations of CH<sub>3</sub>CCl<sub>3</sub>, *J. Geophys. Res.*, *95*, 18,441–18,472, 1990.
- Voldner, E. C., L. A. Barrie, and A. Sirois, A literature review of dry deposition of oxides of sulfur and nitrogen with emphasis on long-range transport modeling in North America, *Atmos. Environ.*, *20*, 2101–2123, 1986.
- Walcek, C. J., R. A. Brost, J. S. Chang, and M. L. Wesely, SO<sub>2</sub>, sulfate, and HNO<sub>3</sub> deposition velocities computed using regional land use and meteorological data, *Atmos. Environ.*, *20*, 949–964, 1986.
- Wesely, M. L., J. A. Eastman, D. H. Stedman, and E. D. Yalvac, An eddy correlation measurement of NO<sub>2</sub>, *Atmos. Environ.*, *16*, 815–820, 1982.
- World Meteorological Organization (WMO), Atmospheric ozone 1985, WMO global ozone research and monitoring project, *Rep. 16*, 648 pp., Geneva, 1985.
- W. L. Chameides, School of Earth and Atmospheric Sciences, Georgia Institute of Technology, Atlanta, GA 30332.
- P. S. Kasibhatla, H. Levy, II, and W. J. Moxim, Geophysical Fluid Dynamics Laboratory, Princeton University, P. O. Box 308, Princeton, NJ 08542.

(Received August 13, 1990;  
revised June 20, 1991;  
accepted June 20, 1991.)